

REFERENCES AND NOTES

- C. T. Kresge *et al.*, *Nature* **359**, 710 (1992).
- J. S. Beck *et al.*, *J. Am. Chem. Soc.* **114**, 10834 (1992).
- A. Monnier *et al.*, *Science* **261**, 1299 (1993).
- Q. Huo *et al.*, *Nature* **368**, 317 (1994).
- Q. Huo *et al.*, *Chem. Mater.* **6**, 1176 (1994).
- A. Firouzi *et al.*, *Science* **267**, 1138 (1995).
- J. Emmer and M. Wiebcke, *Chem. Commun.* **1994**, 2079 (1994).
- The description of surfactant organization in amphiphilic liquid crystal arrays is described in terms of the local effective surfactant packing parameter $g = V/a_0l$, where V is the total volume of the surfactant chains plus any cosolvent organic molecules between the chains, a_0 is the effective head group area at the micelle surface, and l is the kinetic surfactant tail length (Fig. 4). Spherical micelles will form if $g < 1/3$, rodlike micelles if $1/3 < g < 1/2$, vesicles or bilayers if $1/2 < g < 1$, and inverted micelles if $g > 1$. For details, see J. N. Israelachvili, D. J. Mitchell, B. W. Ninham, *Faraday Trans. 2* **72**, 1525 (1976).
- The surfactants were synthesized by reactions of the α,ω -dibromoalkanes with N,N,N -alkyldimethylamine or alkanediyl- α,ω -bis(dimethylamine) with a corresponding bromoalkane for C_{n-s-1} and (3-bromopropyl)trimethylammonium bromide with N,N,N -alkyldimethylamine or bromohexadecane with a corresponding amine for C_{n-s-1} . For the details of the method, see (22).
- The normalized adsorption α_s is obtained from the isotherm on a reference sample and is plotted against relative pressure P/P_0 to obtain a standard α_s curve. The α_s curve can then be used to construct an α_s plot from the isotherm of a test sample. [For details, see S. J. Gregg and K. S. W. Sing, *Adsorption, Surface Area and Porosity* (Academic Press, London, 1982)].
- A common synthesis procedure was applied in our experiments: The surfactant was first dissolved in a basic solution (such as NaOH) or an acidic solution (such as HCl), and then TEOS or another silicate source was added. The resulting mixture was stirred at room temperature for a certain time, and then heated if a high reaction temperature was desired. The solid product was recovered by filtration and dried at room temperature.
- This structure was identified as belonging to the space group $P6_3/mmc$. This assignment was made by x-ray diffraction and by studies of transmission electron microscopy. The absence of certain types of hkl reflections along with the presence of a symmetry center and the finding of a hcp structure (based on the a/c ratio and the analogy of typical hcp structures) were used in this identification. Further details of the crystallographic analysis will be discussed elsewhere (R. Leon, Q. Huo, P. Petroff, G. D. Stucky, in preparation).
- D. Schiferl *et al.*, *Acta Crystallogr. C* **39**, 1151 (1983).
- D. T. Cromer, R. L. Mills, D. Schiferl, L. A. Schwalbe, *Acta Crystallogr. B* **37**, 8 (1981).
- K. Fontell, K. K. Fox, E. Hansson, *Mol. Cryst. Liq. Cryst.* **1**, 9 (1985).
- H. Hagslatt, O. Soderman, B. Jonsson, *Langmuir* **10**, 2177 (1994).
- R. DeLisi and S. Milioto, *Chem. Soc. Rev.* **23**, 67 (1994).
- M. J. Rosen, *Surfactants and Interfacial Phenomena* (Wiley-Interscience, New York, 1989).
- K. S. W. Sing *et al.*, *Pure Appl. Chem.* **57**, 603 (1985).
- P. J. Branton *et al.*, *Faraday Trans.* **90**, 2965 (1994).
- M. R. Bhambhani, P. A. Cutting, K. S. W. Sing, D. H. Turk, *J. Colloid Interface Sci.* **38**, 109 (1972).
- R. Zana *et al.*, *Langmuir* **7**, 1072 (1991).
- E. Alami, H. Levy, R. Zana, *ibid.* **9**, 940 (1993).
- R. Zana and Y. Talmon, *Nature* **362**, 228 (1993).
- In order for one to directly synthesize the bicontinuous cubic ($Ia3d$) phase, the presence of MCM-48 (from use of cetyltrimethylammonium as the template), ethanol (which comes from the silica source TEOS), or a polar organic additive [such as $(CH_3)_2NCH_2CH_2OH$, $N(CH_2CH_2OH)_3$] with fumed silica (Cab-o-Sil) as the silica source is necessary [for details, see (1–3)].
- Funds were provided by the Office of Naval Re-

search (G.D.S. and Q.H.), NSF grant DMR 92-08511 (G.D.S. and Q.H.), Air Products (G.D.S. and Q.H.), Mobil (G.D.S.), and the NSF Science and Technology Center for Quantized Electronic Structures (QUEST) [grant DMR-91-20007 (R.L. and

P.M.F.)]. This work made use of the Materials Research Laboratory Central Facilities supported by NSF award DMR-9123048.

29 November 1994; accepted 8 March 1995

Solar-Like M-Class X-ray Flares on Proxima Centauri Observed by the ASCA Satellite

Bernhard Haisch, A. Antunes, J. H. M. M. Schmitt

Because of instrumental sensitivity limits and stellar distances, the types of x-ray flares observable on stars have been intrinsically much more energetic than those on the sun. Such enormous events are a useful extrapolation of the solar phenomenon if the underlying assumption is correct that they form a continuous sequence involving similar physical processes as on the sun. The Advanced Satellite for Cosmology and Astrophysics (ASCA), with its greater sensitivity and high-energy response, is now able to test this hypothesis. Direct comparison with solar flares measured by the x-ray-monitoring Geostationary Operational Environmental Satellites (GOES) is possible. The detection of flares on Proxima Centauri that correspond to GOES M-class events on the sun are reported.

Geomagnetic storms associated with the largest solar flares can cause communications disruptions and even power outages. For example, the event associated with the X-class flare of 10 March 1989 blacked out the Hydro-Quebec power system (1). Non-negligible radiation exposure of passengers on long commercial flights can result during major events, especially in the auroral latitude zones. Understanding solar flares is therefore of some importance, and the monitoring of solar activity and the development of flare forecasting ability have been long-standing programs in both the U.S. Department of Commerce and Department of Defense (2). Since 1969, the key observational component in this system has been the GOES series of the National Oceanic and Atmospheric Agency (NOAA), which continuously monitor the solar x-ray flux.

Stellar flares have been observed for 20 years to emit x-rays, but the events must be much larger—by as much as a factor of 10^4 —than even the most energetic on the sun in order to be detected across the enormous distances. While stellar “superflares” are of considerable interest, it is equally important to ascertain whether and with what frequency commonplace solar-like events occur on stars. Being able to observe such events is an important test of the working hypothesis that we are dealing with scaled-up versions of the same physical phenom-

non. The Japanese ASCA satellite (3) has now succeeded in such a detection, observing very typical M-class solar-like flares on the next nearest star, Proxima Centauri.

The GOES classification for solar x-ray flares is a linear function of the flux in the ~ 1 to 8 \AA band by which criterion flares are assigned a class of C, M, or X. The satellite also measures a harder spectral component (~ 0.5 to 4 \AA) in which the flux is typically 10 to 100 times weaker. This weakness is a result of the steeply falling thermal emissivity of plasma at flaring temperatures $T > 10^7 \text{ K}$ for wavelengths $\lambda < 2 \text{ \AA}$ (Fig. 1). The plotted spectrum is a simulation based on the plasma emissivity model of Mewe *et al.* (4) applied to a flare differential emission measure, which represents the amount of radiating material at the distribution of temperatures typical for flares (5, 6). For this spectral distribution, the GOES band measures 63% of the actual flux in an ideal 1 to 8 \AA band because the

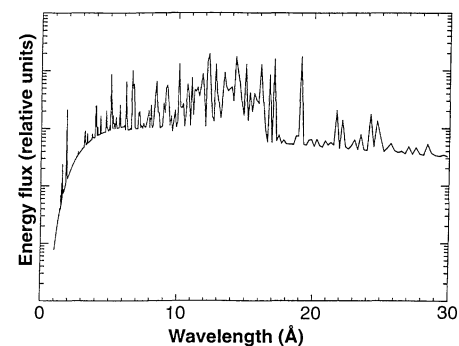


Fig. 1. Spectrum synthesized with the use of a solar flare differential emission measure and a plasma emission code accounting for both lines and continuum radiation in the 1 to 30 \AA region.

B. Haisch, Lockheed Solar and Astrophysics Laboratory, Division 91-30, Building 252, 3251 Hanover Street, Palo Alto, CA 94304, USA.

A. Antunes, Institute of Space and Astronautical Sciences, 3-1-1 Yoshinodai, 229 Sagami-hara-shi, Kanagawa, Japan.

J. H. M. M. Schmitt, Max-Planck-Institut für Extraterrestrische Physik, D-85740 Garching, Germany.

GOES response is not flat in this interval and tails off above and below the nominal limits (7, 8). To differentiate the GOES band from an ideal flat-response one, we hereafter refer to the measured (soft) band as the "GOES-S" band.

A flare of class M1 has a peak power of $L_x = 2.8 \times 10^{25}$ ergs s^{-1} in the GOES-S band, where L_x is the x-ray analog of the astronomical quantity of luminosity. An M2 flare is twice as energetic, and so on. The X class similarly covers the next higher decade; for example, $L_x(X2) = 5.6 \times 10^{26}$ ergs s^{-1} . The degree of solar flaring follows the solar cycle (Table 1) (9). The only cycle for which complete coverage is available is cycle 21, which lasted from June 1976 through August 1986, during which there were 2632 M flares and 172 X flares. Figure 2 shows, as an example, the monthly GOES plot from October 1991, a period of intense solar activity; M and X flares were numerous.

The first detections of stellar x-ray and extreme ultraviolet flares took place in the mid-1970s, although with very poor sensitivity (10, 11). Shortly thereafter, the High-Energy Astronomy Observatory 1 (HEAO-1) satellite succeeded in detecting several flares (12). It was the Einstein Observatory that opened the window on x-ray flares, and one of the most detailed light curves of such an event was observed on 20 August 1980 on Proxima Centauri as part of a coordinated program with the International Ultraviolet Explorer (13). The most

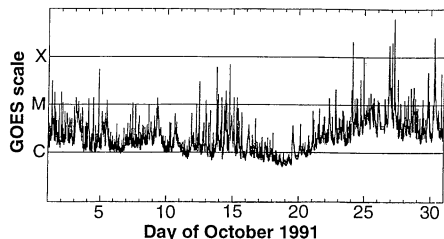
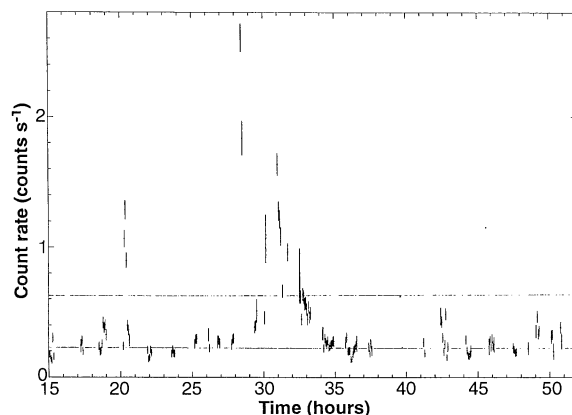


Fig. 2. The monthly GOES plot from October 1991, a period of intense solar activity showing numerous M and X flares.

Fig. 3. ASCA x-ray light curve for Proxima Centauri summed over all four detectors. The lower line shows the average quiescent summed count rate; the top line indicates the M1 flare level above the quiescent emission.



detailed view of a nonsolar flare can be had from the nearest nonsolar site of such activity, which turns out to be Proxima Centauri, at a distance of 1.3 pc. This star is an extremely faint dm5.5e companion to the first-magnitude α Cen binary. Proxima is at such an extreme distance from its companions α Cen A and B that it is not certain whether it is actually bound to the system; its separation in the sky is $>2^\circ$ (14).

Further flare observations of Proxima Centauri were made by the Exosat Observatory (15). Then in 1990, with the launch of ROSAT, a new opportunity arose for such measurements (16). However, the passbands of all these observatories differ significantly from that of GOES-S: ~ 3 to 60 \AA for the Einstein Observatory Imaging Proportional Counter; ~ 6 to 300 \AA for the Exosat Low Energy Telescope; and ~ 6 to 120 \AA for the ROSAT Position Sensitive Proportional Counter. The ASCA observatory, launched 20 February 1993, is sensitive to more energetic x-rays (~ 1 to 24 \AA) and, even at overlapping wavelengths, has significantly more effective area than the previous telescopes [see figure 2 in (3)]. The lower detection threshold and the fact that the ASCA band overlaps entirely with the GOES-S band thus afford a direct comparison between commonplace flares on Proxima Centauri and on the sun.

Proxima Centauri was the target of a National Aeronautics and Space Administration (NASA) Guest Observation with ASCA on 18 to 20 March 1994 that lasted for 23 satellite orbits and yielded about 50,000 s of good data. Observations were carried out with four identical grazing-incidence x-ray telescopes and two different pairs of detectors: two charge-coupled device (CCD)-camera solid-state imaging spectrometers (SIS) and two gas scintillation imaging proportional counters (GIS) (3). The data (Fig. 3) were divided into quiescent and flare intervals, and spectral analysis was carried out according to standard plasma emission models tailored to the ASCA instruments. It is customary to at-

tempt a two-temperature (2T) fit: Generally, a low- T component is interpreted as the average (that is, the most common) temperature, and a high- T component indicates the approximate peak temperature. The statistically best 2T fit for the aggregate of the flare emission was $T_1 \sim 7.3 \text{ MK}$ and $T_2 \sim 44 \text{ MK}$. A formal 2T fit for the quiescent interval was attempted as well, but only the cooler component appears credible. We take the obtained $T_1 \sim 6.1 \text{ MK}$ as representative of the nonflaring coronal emission (17).

We have calibrated the flares relative to the GOES-S band using the solar flare differential emission measure (5, 6) that yields the spectrum in Fig. 1 (18). Calibrated to the SIS response, an M1 flare having solar differential emission measure at the distance of Proxima Centauri would yield 0.1 count s^{-1} in each SIS telescope-detector system. From spectral simulation, it is expected that the GIS would be about half as sensitive to flare radiation. This is indeed the case: During this observation, the average count rates during flare-enhanced intervals showed an SIS to GIS ratio of 1.94 (19). Thus, for the total summed flare signal in all four instruments, an enhancement of 0.3 count s^{-1} would correspond to an M1 flare.

The summed quiescent background was 0.23 count s^{-1} (Fig. 3, lower line). The top line in Fig. 3 indicates an M1 event level above quiescence. It is possible that the

Table 1. Yearly rate of solar M and X flares. The peaks in 13-month averaged, smoothed sunspot number were in November 1968, December 1979, and July 1989 (solar cycles 20, 21, and 22, respectively). These correlate well but not precisely with the flare rate maxima.

Year	M flares	X flares
1969	352	41
1970	534	53
1971	120	6
1972	146	15
1973	80	8
1974	77	15
1975	18	1
1976	14	3
1977	48	4
1978	264	21
1979	452	29
1980	496	21
1981	506	38
1982	606	42
1983	105	6
1984	114	7
1985	17	2
1986	23	2
1987	29	0
1988	193	21
1989	618	59
1990	273	17
1991	590	54
1992	206	10
1993	75	0
1994	25	0

quiescent emission was the cumulative result of many ongoing events of class C or even lesser energy, but this issue of whether coronal heating is entirely the result of flare-like activity or has any steady component is an open issue even for the sun (20)

During solar maximum, the number of M flares per month is ~ 50 , that is, ~ 1.7 per day. During this observation, Proxima Centauri was at least as active as the sun at maximum. It is important to put this in perspective for such a faint dwarf M star: The bolometric luminosity (mainly in the optical and infrared) of Proxima Centauri is only 6.7×10^{30} ergs s^{-1} (21), less than 1/500 that of the sun. The total x-ray luminosity at all wavelengths for the most energetic events on Proxima Centauri observed by ASCA and ROSAT is $L_x \sim 3 \times 10^{27}$ to 6×10^{27} ergs s^{-1} . This amounts to an instantaneous perturbation on the order of 0.1% of the total thermonuclear power of the star.

Observation of ordinary M-class flare events on Proxima Centauri indicates that the assumption that flares on the sun and on other stars are scaled versions of the same process is fundamentally sound. It remains a challenge to understand both how flares can, in an absolute sense, exceed those on the sun by up to four orders of magnitude on such extremely active stars as T Tauris (22) and RS CVn systems (23), and in a relative sense on such faint dwarf M stars as Proxima Centauri.

- Giampapa and J. A. Bookbinder, Eds., vol. 26 of the *ASP Conference Series* (Astronomical Society of the Pacific, San Francisco, 1992), pp. 83–92.
17. The formal fits for the flare are $kT_1 = 0.63 \pm 0.01$ keV (k is Boltzmann's constant) with an emission measure $EM_1 = 5 \times 10^{49}$ cm^{-3} and $kT_2 = 3.83 \pm 0.67$ keV with $EM_2 = 3 \times 10^{49}$ cm^{-3} . These fits were calculated assuming a column density of hydrogen N_H conservatively fixed at 3×10^{19} cm^{-2} , resulting in a reduced $\chi^2 = 2.3$. For the quiescent intervals, $kT_1 = 0.53$ keV with $EM_1 = 10^{49}$ cm^{-3} and $kT_2 > 4$ keV with $EM_2 = 9 \times 10^{48}$ cm^{-3} (reduced $\chi^2 = 2.9$). In both cases, fitting was hindered by low count rates above 6 keV, and in particular, we do not consider the quiescent kT_2 fit to be credible. These temperatures are marginally statistically hotter than the Einstein Observatory determinations in (13).
 18. A continuous distribution of temperature for the flaring plasma is likely to be more realistic than the two isolated temperatures T_1 and T_2 . Moreover, the temperature of the DEM (differential emission measure) maximum and the highest temperature of the DEM are similar to T_1 and T_2 of the flare.
 19. The average count rates for the flare intervals are

- $SIS_a = 0.331$, $SIS_b = 0.258$, $GIS_a = 0.136$, and $GIS_b = 0.168$ counts s^{-1} . The absolute values are quite dependent on the choice of flare interval; it is the ratio of 1.94 that is important. For the quiescent intervals, they are $SIS_a = 0.071$, $SIS_b = 0.063$, $GIS_a = 0.048$, and $GIS_b = 0.050$ counts s^{-1} .
20. See L. Acton *et al.*, *Science* **258**, 618 (1992) for the Yohkoh view on this.
 21. J. A. Frogel *et al.*, *Publ. Astron. Soc. Pac.* **84**, 581 (1972).
 22. Th. Preibisch, H. Zinnecker, J. H. M. M. Schmitt, *Astron. Astrophys.* **279**, L33 (1993).
 23. R. Ottmann and J. H. M. M. Schmitt, *ibid.* **283**, 871 (1994).
 24. We wish to acknowledge the support of the NASA ASCA Guest Observer Program (contract S-14646-F, B.H. was principal investigator) and the Institute of Space and Astronautical Sciences ASCA Guest Observer Program under whose auspices these observations were carried out. We thank D. Speich of NOAA for providing solar flare data and G. Linford of Lockheed for GOES data plots.

21 November 1994; accepted 24 March 1995

Beryllium-10 Dating of the Duration and Retreat of the Last Pinedale Glacial Sequence

J. C. Gosse,* J. Klein, E. B. Evenson, B. Lawn, R. Middleton

Accurate terrestrial glacial chronologies are needed for comparison with the marine record to establish the dynamics of global climate change during transitions from glacial to interglacial regimes. Cosmogenic beryllium-10 measurements in the Wind River Range indicate that the last glacial maximum (marine oxygen isotope stage 2) was achieved there by $21,700 \pm 700$ beryllium-10 years and lasted 5900 years. Ages of a sequence of recessional moraines and striated bedrock surfaces show that the initial deglaciation was rapid and that the entire glacial system retreated 33 kilometers to the cirque basin by $12,100 \pm 500$ beryllium-10 years.

REFERENCES AND NOTES

1. B. Haisch, K. T. Strong, M. Rodonò, *Annu. Rev. Astron. Astrophys.* **29**, 275 (1991); see also the cause and effect discussion in J. T. Gosling, *J. Geophys. Res.* **98**, 18937 (1993); H. Hudson, B. Haisch, K. T. Strong, *ibid.* **100**, 3473 (1995); J. T. Gosling, *ibid.*, p. 3479.
2. C. Sawyer, J. W. Warwick, J. T. Dennett, *Solar Flare Prediction* (Colorado Associated Univ. Press, Boulder, CO, 1986).
3. Y. Tanaka, H. Inoue, S. S. Holt, *Publ. Astron. Soc. Jpn.* **46**, L37 (1994).
4. R. Mewe, E. H. B. M. Gronenschild, G. H. J. van den Oord, *Astron. Astrophys.* **62**, 197 (1985).
5. M. E. Bruner and R. W. P. McWhirter, *Astrophys. J.* **326**, 1002 (1988).
6. K. P. Dere and J. W. Cook, *ibid.* **229**, 772 (1979).
7. R. F. Donnelly, R. N. Grubb, F. C. Cowley, *NOAA Tech. Memo. ERL SEL-48* (1977).
8. R. J. Thomas, R. Starr, C. J. Crannell, *Solar Phys.* **95**, 323 (1985).
9. D. Speich, private communication.
10. J. Heise *et al.*, *Astrophys. J.* **202**, L73 (1975).
11. B. Haisch *et al.*, *ibid.* **213**, L119 (1977).
12. S. M. Kahn *et al.*, *ibid.* **234**, L107 (1979).
13. B. M. Haisch *et al.*, *ibid.* **267**, 280 (1983).
14. R. Mathews and G. Gilmore, *Mon. Not. R. Astron. Soc.* **261**, L5 (1993). If Proxima is bound, the semi-major axis of its orbit is at least 13,000 astronomical units (AU), with an orbital period $\geq 10^6$ years. If Proxima is not bound, then there would be no justification for assuming it to be coeval with α Cen A and B, and we would thus have no way of associating its flare activity with its age.
15. B. Haisch, C. J. Butler, B. Foing, M. Rodonò, M. S. Giampapa, *Astron. Astrophys.* **232**, 387 (1990).
16. J. H. M. M. Schmitt, in *Cool Stars, Stellar Systems, and the Sun: Seventh Cambridge Workshop*, M. S.

Alpine glacial systems are more responsive than large continental ice sheets to changes in temperature and precipitation. Chronologies of alpine morainal sequences therefore offer the possibility of providing records of Pleistocene climate variations that have higher resolution than do global ice volume records (for example, marine isotopic data). Establishing tight time constraints on the age of morainal deposition has been difficult. Determining how long a glacier has occupied its terminal position (that is, the duration of the glacial maximum) has been even harder. Here, we use measurements of cosmogenic ^{10}Be in quartz exposed in boulders on alpine moraines to reconstruct the complete Pinedale glacial history of the Fremont Lake basin in Wyoming.

During the last major glaciation, a large ice cap on the Wind River Range fed outlet

glaciers in the Fremont Lake basin located on the western piedmont of the Wind River Mountains in west-central Wyoming (Fig. 1). The Fremont Lake basin is the type locality for the Pinedale glaciation (1, 2), corresponding to the late Wisconsinan-age (marine oxygen isotope stage 2) glaciation in the Rocky Mountains. The type-Pinedale glacial deposits have been extensively studied, and other deposits throughout North America and South America have been correlated to the type-Pinedale moraines. A precise chronology for the advance and retreat of Pinedale glaciers would provide the basis for addressing the synchronicity of glacial onset and termination in the Northern and Southern hemispheres.

There are only a few dates that tightly constrain the timing or duration of the last Pinedale glacial maximum (LPGM). A minimum age of the LPGM at the type locality is limited by two radiocarbon dates of 6100 ± 100 and 9300 ± 80 ^{14}C years before present (B.P.) [6800 ± 100 and $10,000 \pm 50$ years, calibrated radiocarbon ages (3)] from the bottom of a bog (4). Approximately 33.8 km north-northwest of Fremont Lake, a vegetational change asso-

J. C. Gosse, Earth and Environmental Sciences, Lehigh University, Bethlehem, PA 18015, USA, and ESS-1 MS D462, Los Alamos National Laboratory, Los Alamos, NM 87545, USA.

J. Klein, B. Lawn, R. Middleton, Department of Physics, University of Pennsylvania, Philadelphia, PA 19104, USA. E. B. Evenson, Earth and Environmental Sciences, Lehigh University, Bethlehem, PA 18015, USA.

*To whom correspondence should be addressed.